Iraqi Journal of Veterinary Sciences

www.vetmedmosul.com

A comparative histopathological study of pancreas, intestine, and liver of experimentally induced diabetes in rats

M.A. Ali[1] and N.G. Mustafa[2]

[1]Nineveh Agriculture Directorate, [2]Department of Physiology, Biochemistry and Pharmacology, College of Veterinary Medicine, University of Mosul, Mosul, Iraq.

Article information

Article history:
Received March 20, 2023
Accepted June 7, 2023
Available online September 15, 2023

Keywords:
Alloxan
Diabetes
Diet
Rats
Streptozotocin

Correspondence:
N.G. Mustafa
nashaat74@uomosul.edu.iq

Abstract

For several decades, experimentally induced diabetes has been a cornerstone in the research field of this syndrome. Various methods have been applied to induce diabetes, such as chemical induction (by alloxan or streptozotocin), surgical induction (by pancreatectomy), special high-carbohydrate diets, and genetically diabetic animals (such as ob/ob mice). However, few studies have investigated the histopathological changes associated with different induction methods and compared these approaches. Therefore, we aim to investigate the common induction methods (alloxan, streptozotocin, and special diets) in adult male rats and compare the histopathological changes resulting from each method. Serum glucose monitoring confirms the induction of diabetes, and histopathological studies reveal a wide range of lesions in the pancreas (a significant reduction in the diameter and number of Langerhans islets), liver (necrosis, acute cell swelling, the presence of cellular debris, karyolysis, and vacuolar degeneration), and intestine (a significant reduction in the length and width of intestinal villi, and a diminished number of goblet cells). In conclusion, various approaches to induce diabetes in rat result in a wide range of histopathological lesions. Further investigation is needed to determine the most suitable method to induce diabetes and to assess the implications of these histopathological changes on the efficacy of treatments for diabetes.

DOI: 10.33899/IJVS.2023.138343.2791,

Introduction

Diabetes Mellitus (DM) is one of the most critical chronic metabolic disorders caused by a complete or partial lack of insulin, leading to a default in the metabolism of carbohydrates, lipids, and proteins (1,2). Whether in humans or pet animals, DM has received consistent attention for many decades due to its widespread incidence (particularly in dogs and cats) and the fact that it affects almost all body systems and has wide variety of manifestations. Hyperglycemia stands as the main symptom, in addition to polydipsia, polyuria, and polyphagia (3-5). Two main types of diabetes are recognized: insulin-dependent (type 1) diabetes, which results from the destruction of Langerhans beta cells in the pancreatic islets, and non-insulin-dependent (type 2) diabetes, which is usually due to a default of insulin secretion and/or the presence of insulin resistance (6,7). Although absolute or relative insulin insufficiency predominates, there is a tremendous variation in the etiology and pathophysiology of diabetes (8). Thus, the long and ongoing journey of DM research began many decades ago (9). These researches depend mainly on the experimental induction of DM in laboratory animals with various chemicals such as streptozotocin, alloxan, and other specific substances (10,11). In experimentally induced diabetes, rodents are preferred choice for apply because of their body size, they have a calm behavior, which lets easy handling by researchers, as well as significantly lower food and housing costs (12). Several research models of diabetic animals have been established such as utilizing of the streptozotocin (STZ)

or alloxan model (T1DM), partial or complete removal of pancreas, model of special diet of high-fat (HF), and fructose feeding model (T2DM). Parenteral streptozotocin and alloxan (urea derivative) are the mainly applied chemicals to induction of diabetes in laboratory animals (13). On the other hand, a few studies were done to evaluate the histopathological changes in different induction approaches (14-16).

In our current study, alloxan, streptozotocin, and special food were used to induce diabetes mellitus in rats, then different target body organs were explored and evaluated by histopathological study.

Materials and methods

Ethical approve

The University of Mosul, College of Veterinary Medicine's Animal Care and Use Committee approved each all the experimental protocols (Um.VET.2022.063 on 17/12/2021).

Experimental animals

Forty-eight adult male albino laboratory rats, aged 3-4 months and weighing between 250-400 gm, were used in this study. The experiments were conducted in the laboratory animal house at the College of Veterinary Medicine, University of Mosul. The rats underwent a veterinary examination and were monitored for general health, with appropriate environmental conditions including well-ventilated rooms, a temperature of 22 ± 2ºC, and regular 12-hour light-dark cycles. The rats were housed in special plastic cages measuring 30x20x17 cm. All experiments were conducted the guidelines for the care and use of laboratory animals of the National Institute of Health (NIH) (17). One group of rats was induced with diabetes using white bread and saturated sugar solution, while the other groups were induced using other methods. The rats were treated according to laboratory animal care instructions (17) and were divided into the following groups; Control group have eight rats were not treated with any chemicals or special diet. The level of glucose was measured frequently using the Accu-Chek® device (Roche, Germany). Alloxan group have eight rats were injected subcutaneously with alloxan at a dose of 200 mg/kg body weight after 12 hours of fasting (18). The level of glucose was measured frequently using the Accu-Chek® device (Roche, Germany). Streptozotocin (STZ) group have eight rats were injected subcutaneously with STZ at a dose of 50 mg/kg body weight after 12 hours of fasting, weekly for one month (19). High fructose with food and alloxan group have eight rats were injected subcutaneously with alloxan at a dose of 200 mg/kg body weight and given white bread as their food with a saturated fructose solution of 40% W/V (20). High fructose with food and STZ group have eight rats were injected subcutaneously with STZ at a dose of 50 mg/kg body weight and given white bread as their food with a saturated fructose solution of 40% W/V. Alloxan with STZ group have eight rats were injected with a single dose of 100 mg/kg alloxan+5 mg STZ after 12 hours of fasting.

Histopathological study

All animals were sacrificed for histological examination. The pancreas, liver, and small intestine were removed and fixed in a 10% buffered neutral formalin solution (21). Small samples were taken from each organ and were treated with traditional histological methods, including dehydration in ethyl alcohol, clearing in xylol, and embedding in hot paraffin wax. The wax blocks were sectioned (5 µm) using a microtome, and the slides were stained with ordinary Harris hematoxylin and eosin (aqueous) (22). The histopathological samples were examined using an optical microscope with two lenses (OLYMPUS, Japan) and photographed using an OMAX 18MP LAPAN camera (China).

Statistical analysis

The Statistical Package for Social Sciences (SPSS, version 25) was used for statistical analysis. The experimental data were presented as mean values with their standard deviation (mean ± SD) and analyzed using a one-way analysis of variance (ANOVA). A probability level of $P \leq 0.05$ was considered statistically significant (23).

Results

The elevated blood glucose concentration observed in all treated groups (Table 1) was significant ($P \leq 0.05$) and indicates the presence of diabetes. Table 2 and figures 1-6, present the dimensions of histological architectures of the pancreas, showing a significant decrease in the number of islets of Langerhans in all treated groups, with the lowest observed in the alloxan group at a dose of 200 mg/kg (4.4 ± 0.24 number/10x field). There was a significant variance ($P \leq 0.05$) between the treated and control groups. Additionally, table 1, shows a significant decrease in the diameter of Langerhans islets, with the lowest observed in the group treated with 100 mg/kg of alloxan and 5 mg/kg of STZ (36.28±2.54 µm). Histological sections confirmed pathological changes, characterized by necrosis and a decrease or loss of Langerhans islet cells, as well as degeneration and necrosis of pancreatic acinar cells. The deposition of acidic protein materials was also observed in the lumen of the lobe ducts.

Microscopic examination of the liver demonstrated that the control group (Figure 7) had a normal shape and arrangement of hepatocytes, as well as clear sinusoids and portal area. In the treated groups (Figures 8-12), there was a characteristic hepatocyte coagulative necrosis, acute cell swelling, presence of cellular debris, karyolysis, and vacuolar degeneration. In addition, there were few infiltrations of inflammatory cells and confirmed congestion

of the central vein. Congestion of the portal vein, cloudy degeneration, thromboembolic necrosis, and expansion in sinusoids were also observed. However, no fatty changes in the liver were detected.

On the other hand, table 3 illustrate that there was a significant (P≤0.05) decrease in the length of intestinal villi in the group receiving 50 mg/kg STZ with a high-fructose diet, compared to the group on a high-fructose diet alone. The villi length in the former was 267.38±13.41 µm, while in the latter it was 269.48±10.21 µm. Additionally, there was a significant increase in the width of the villi between the groups, with the greatest width observed in the group receiving 200 mg/kg of alloxan and the group receiving 50 mg/kg of STZ, at 212.78 ± 6.17 and 200 ± 9.80, respectively. A significant increase in the number of goblet cells, was also observed, with the highest count in the group receiving 200 mg/kg alloxan, at 212.78 ± 6.17. There was a significant difference (P≤0.05) between the treated groups and the control group.

Regarding the intestinal tissues (Figure 13), the control group, displayed a regular histological architecture of a cross-section of the intestine with villi and crypts of Lieberkühn, goblet cells, the tunica mucosa, and the tunica muscularis. In contrast, the treated groups (Figures 14-16) showed a shortening of the villi length and thickness of the mucous layer of the intestine, necrosis of the cells lining the intestine, infiltration of inflammatory cells, an increase in the number of goblet cells, and desquamation of the cells lining the villi in the lumen. Additionally, there was severe necrosis in the mucous layer, and necrosis of the cells lining the crypts.

Table 1: Serum glucose concentration in all experimental groups

Groups	Serum glucose (mg/dl)
Control	75.66±6.2e
Alloxan	166.87±12.4c
STZ	184.32±5.5c
High fructose+food+alloxan	204.80±11.2b
High fructose+food+STZ	244.79±9.7a
Alloxan+STZ	231.4±10.8a

Letters in each column represent a significant difference (P≤0.05) when compared with the control group.

Table 2: Pancreas histopathological diameters in control and treated groups

Groups	No. of islet/10x field	diameter of the islet
Control	5±0.32 a	152.86±14.5a
Alloxan	4.4±0.24 b	87.12±4.81c
STZ	3.4±0.51 c	70±2.32c
High fructose+food+alloxan	4.8±0.73b	113.49±14.83b
High fructose+food+STZ	2.2±0.37d	47.96±3.74e
Alloxan+STZ	2±0.52d	36.28±2.54 e

Letters in each column represent a significant difference (P≤0.05) when compared with the control group.

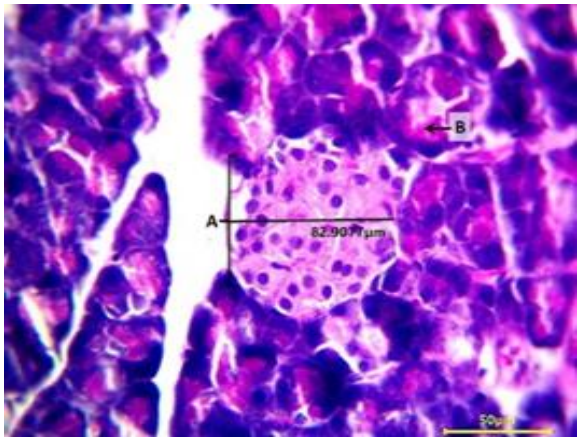

Figure 1: Micrographs of pancreas tissue, control group: Normal histological features with intact islets of Langerhans (A), pancreatic auricles (B), and lobar ducts (C). H and E stain, 100X.

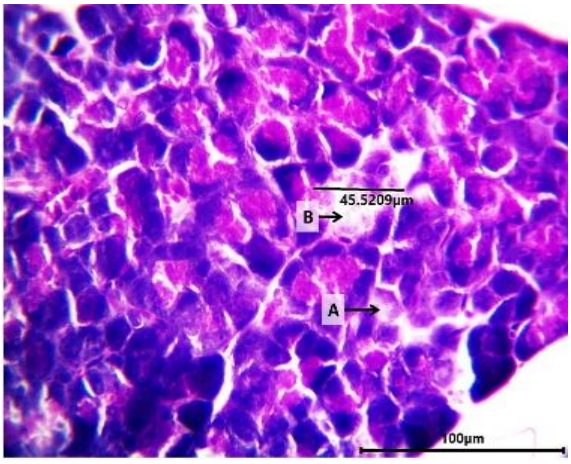

Figure 2: Micrographs of pancreas tissue, alloxan group: Necrosis and loss of islet cells (A) and degeneration and necrosis of pancreatic acinar cells (B) with measured islet diameter (µm). H and E stain, 400X.

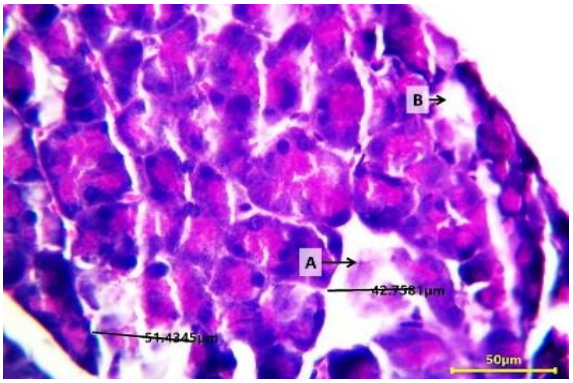

Figure 3: Micrographs of pancreas tissue, STZ group: Necrosis and loss of islet cells and pancreatic acinar cells (A and B) with measured islet diameter (µm). H and E stain, 400X.

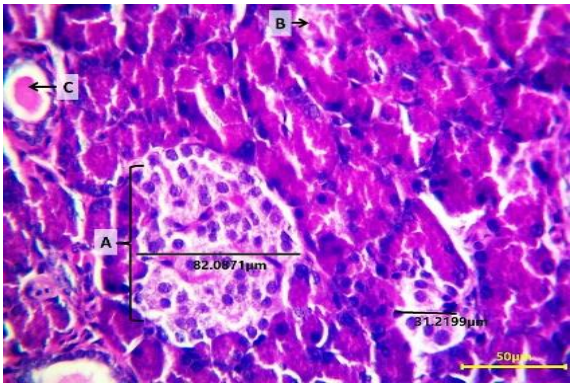

Figure 4: Micrographs of pancreas tissue, high fructose+food+alloxan group: Normal features of islets of Langerhans (A) with slight degeneration of pancreatic acinar cells (B). H and E stain, 100X.

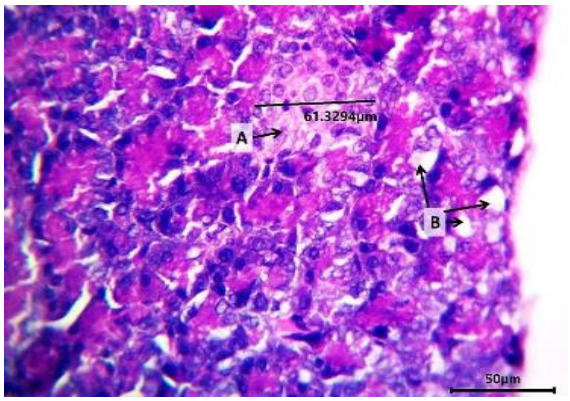

Figure 5: Micrographs of pancreas tissue, high fructose+food+STZ group: Atrophy of pancreatic tissue (↔), necrosis of some islet cells (A), severe vacuolar degeneration and necrosis of pancreatic acinar cells and lobular ducts (B and C) with vascular congestion (D). H and E stain, 100X.

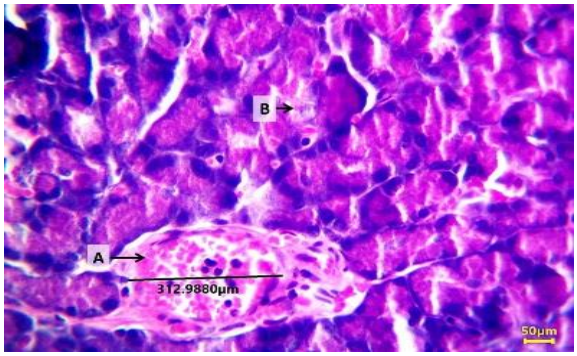

Figure 6: Micrographs of pancreas tissue, alloxan+STZ group: Necrosis of islet cells with deposition of acidic proteases (A) and degeneration and necrosis of pancreatic acinar cells (B) with measured islet diameter (µm). H and E stain, 400X.

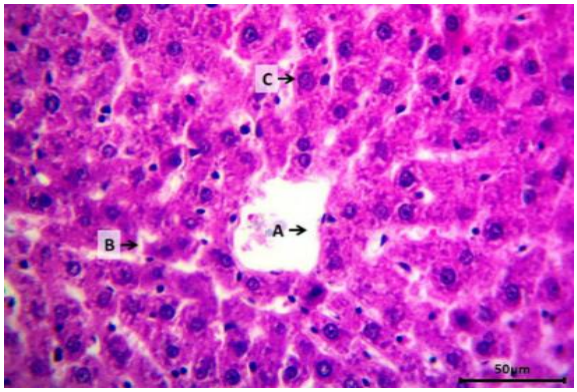

Figure 7: Micrographs of liver tissue, control group: normal histological features observed in liver tissue including a central vein (A), sinusoids (B), and hepatocytes (C). H and E stain, 400X.

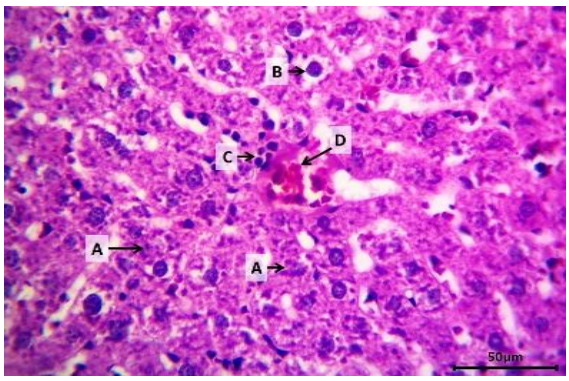

Figure 8: Micrographs of liver tissue, alloxan group: necrosis of hepatocytes, presence of cellular debris and broken nuclei (A), vacuolar degeneration (B), infiltration of inflammatory cells (C), and congestion of the central vein (D). H and E stain, 400X.

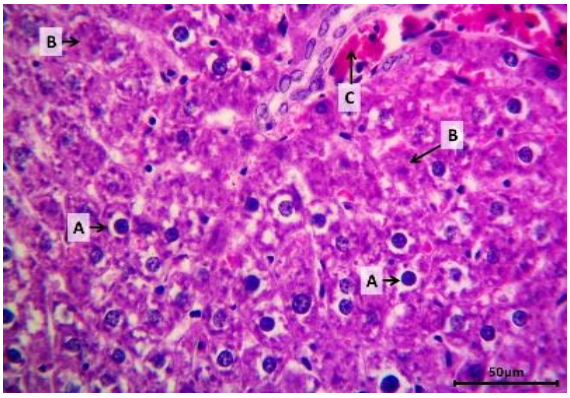

Figure 9: Micrographs of liver tissue, STZ group: vacuolar degeneration of hepatocytes (A) and coagulative necrosis in the portal region (B) with portal vein congestion (C). H and E stain, 400 X.

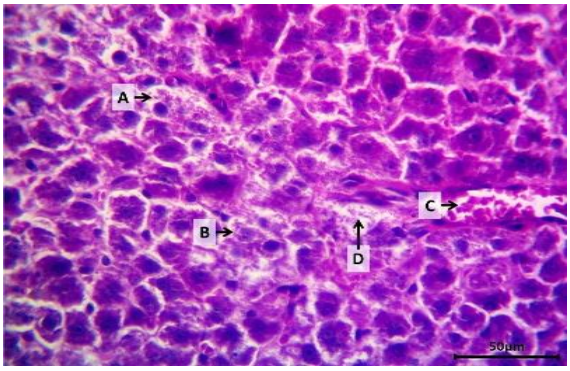

Figure 10: Micrographs of liver tissue, high fructose+food+alloxan group: cloudy degeneration of hepatocytes (A), coagulative necrosis (B), central vein congestion (C), and sinusoidal dilatation (D). H and E stain, 400 X.

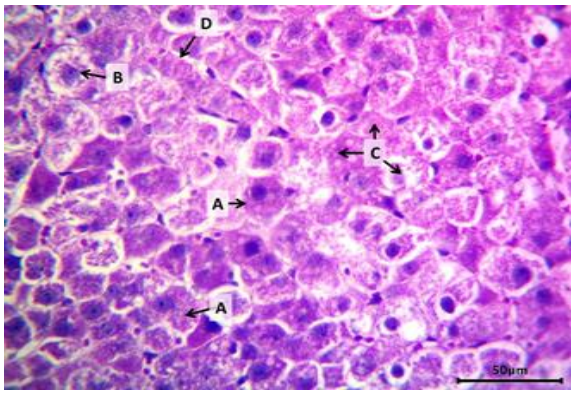

Figure 11: Micrographs of liver tissue, high fructose+food+STZ group: acute cell swelling (A), cloudy degeneration (B), necrosis of hepatocytes (C), and stenosis of the sinusoids (D). H and E stain, 400X.

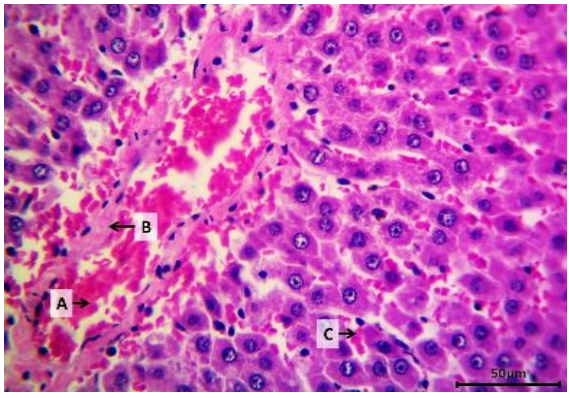

Figure 12: Micrographs of liver tissue, alloxan+STZ group: slight vacuolar degeneration (A), slight cloacal degeneration of hepatocytes (B), central venous congestion (C), and sinusoids (D). H and E stain, 400X.

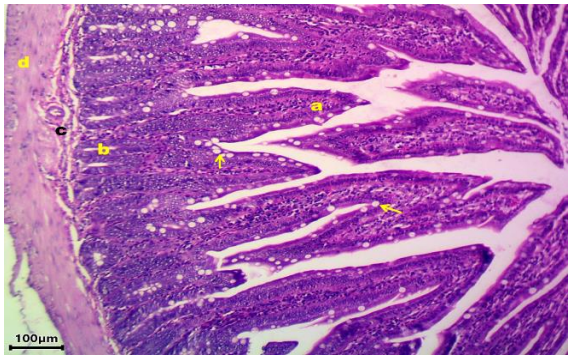

Figure 13: Micrograph of intestine, control group: a cross-section of the intestine showing the normal structure of the intestinal villi (a), Lieberkühn's folds (b), the tunica submucosa (c), and the tunica muscularis (d). H and E stain, 40X.

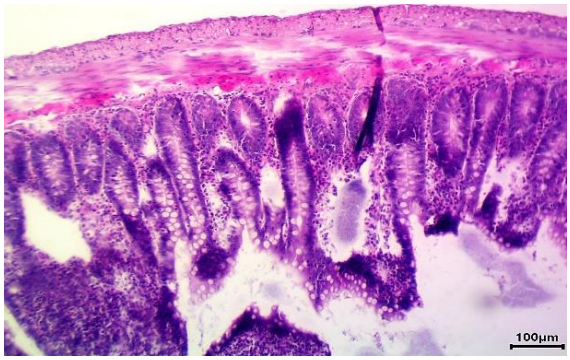

Figure 14: Micrograph of intestine, alloxan group: showing a decrease in the length of the villi and the thickness of the intestinal mucosa (a), necrosis of the cells lining the intestine (b), and infiltration of inflammatory cells (c). H and E stain, 100X.

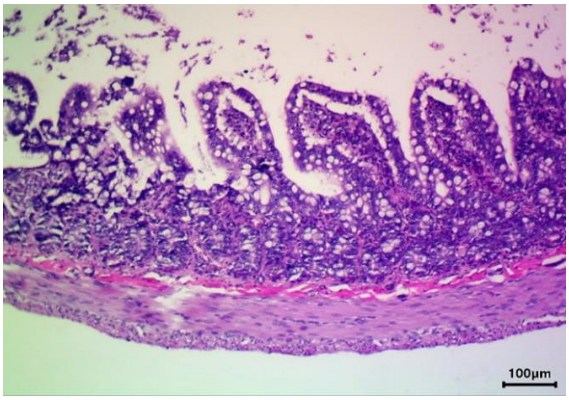

Figure 15: Micrograph of intestine, high fructose+food+STZ group: showing a decrease in the length of the villi and the thickness of the intestinal mucosa (a), necrosis in the mucosal layer (b) and the muscular layer (c), and an increase in the number of goblet cells (arrow). H and E stain, 100X.

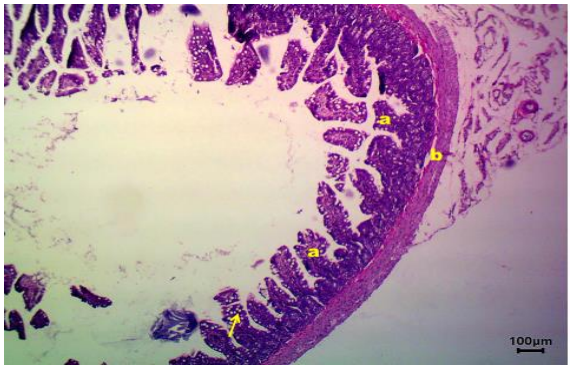

Figure 16: Micrograph of intestine, alloxan+STZ group: showing a decrease in the length of the villi and the thickness of the intestinal mucosa (a), necrosis in the mucosal layer (b) and the muscular layer (c), and an increase in the number of goblet cells (arrow). H and E stain, 100X.

Table 3: Small intestine histopathological diameters in control and treated groups

Groups	Length of villi	Width of villi	No. of goblet cell
Control	933.94±50.45 a	106.46±6.28 b	16.41±1.36 c
Alloxan	435.08±36.72 c	212.78±6.17 a	31±0.94 a
STZ	442.66±21.82 c	200±9.80 a	16.41±1.36 c
High fructose+food+alloxan	269.48±10.21 e	112.02±10.95 b	29.22±1.8 a
High fructose+food+STZ	267.38±13.41 e	138.88±23.40 b	30.62±1.50 a
Alloxan+STZ	431.88±42.24 c	81.73±9.71 e	29.24±0.86 a

Letters in each column represent a significant difference (P≤0.05) when compared with the control group.

Discussion

In this study, diabetes mellitus was successfully induced in all treated groups, with alloxan inducing DM in 70% of animals and 30% dying within 24 hours due to shock. The characteristic feature of diabetes, hyperglycemia, was demonstrated significantly. The establishment of diabetes in rats in this study may be attributable to the definite, irreversible toxic impacts of alloxan on the pancreatic beta cells, which represent only 20% of islet cells (24,25). Inside the body, alloxan is rapidly reduced to dialuric acid, which later undergoes auto-oxidation, forming a significant quantity of superoxide anion ($O2^{-}$), hydroxyl free radicals ($H2^{-}$), and hydrogen peroxide (H_2O_2). These reactive species of oxygen are assumed to inflict alloxan-based violence on the beta cells (26-29).

On the other hand, STZ preferentially accumulates in the beta cells of the pancreas through the glucose transporter (GLUT2) (30). STZ then splits into glucose and methylnitrosourea, with the latter responsible for alkylating properties that cause irreversible deterioration of macromolecules, particularly mitochondrial DNA (mtDNA). This leads to damage to various metabolic signaling pathways, and ultimately the beta cells become readily vulnerable to cell death, causing depression in insulin production (31,32).

However, experimentally induced diabetes is believed to cause a variety of pathological changes in different tissues, including the small intestine. Simonyan *et al.* (33) documented that the diabetic rat intestine has an elevated level of oxidative stress biomarkers. The authors also demonstrated that the diabetes rat intestine has a significant four-fold elevation in lipid peroxidation, as well as increased levels of catalase and SOD, with depression of glutathione peroxidase (34,35). Overall, these biochemical fluctuations appear to be responsible for the histopathological changes observed in all treated groups in our study.

On the other hand, previous studies (36,37) have documented that experimentally induced diabetes in rats can lead to various modifications in liver tissue that are similar to chronic liver diseases in humans, including degeneration and fibrosis. These changes affect the hepatic portal areas and sinusoids, and researchers have also studied the ultrastructural deviations in hepatic cells, particularly rough endoplasmic reticulum, and mitochondria. Goel (38) reported that after 5 days of induction of experimental diabetes in fish, there was necrosis in hepatocytes, and he suggested that alloxan may alter signaling pathways of

metabolism, especially by inhibiting certain enzyme activity. Meanwhile, Kume *et al.* (36) found that STZ-induced diabetes in mice causes clear changes such as hepatocyte hypertrophy and the participation of intracellular particles. Lucchesi *et al.* (39) showed that rat liver cells undergo changes after the induction of diabetes, including enlarged mitochondria and diminished rough endoplasmic reticulum. Notably, the administration of insulin and the reversal of hyperglycemia (particularly after 2 weeks of diabetes induction) can restore these changes to a normal state. Therefore, these changes in the first 2 weeks seem to be due to insulin deficiency and hyperglycemia, rather than the direct cytotoxic effect of alloxan or STZ on the liver (40). Furthermore, the severity of histopathological lesions in the rat liver appears to be strongly related to the time course of diabetes, with the severity increasing over time, particularly after 24 weeks of uncontrolled hyperglycemia. This includes enlargement of sinusoids, focal fatty degenerations, hepatocyte vacuolization, and occasionally infiltration of mononuclear inflammatory cells with periportal fibrosis (40). Steatohepatitis was not observed in this study, and this may be due to the relatively short duration between the induction of diabetes and the end of the experiment, which was insufficient to cause fatty changes in the liver.

Conclusion

Different approaches applied to induce diabetes in rats lead to a wide range of histopathological lesions, and according to the detailed aim of each study, individual approach should be used. A further experimental investigation is needed to determine the most appropriate method to induce diabetes and to assess the implications of these histopathological changes on the effectiveness of treatments for diabetes.

Acknowledgment

The authors of this study would like to express their gratitude to the University of Mosul, College of Veterinary Medicine, for their non-financial support in this work.

Conflict of interest

There is no conflict of interest, according to the authors.

References

1. ElSayed NA, Aleppo G, Aroda VR, Bannuru RR, FM, Bruemmer D, Collins BS, Cusi K, Das SR, Gibbons CH, Giurini JM, Hilliard ME, Isaacs D, Johnson EL, Kahan S, Khunti K, Kosiborod M, Leon J, Lyons SK, Murdock L, Perry ML, Prahalad P, Pratley RE, Seley JJ, Stanton RS, Sun JK, Woodward CC, Young-Hyman D, Gabbay RA. Summary of revisions: Standards of care in diabetes. Diabetes. 2023;46(1):S5-S9. DOI: 10.2337/dc23-srev
2. Kee OT, Harun H, Mustafa N, Abdul Murad NA, Chin SF, Jaafar R, Abdulla N. Cardiovascular complications in a diabetes prediction model using machine learning: A systematic review. Cardiovasc Diabetol. 2023;13(2023):13-22. DOI: 10.1186/s12933-023-01741-7
3. Laios K, Karamanou M, Saridaki Z, Androutsos G. Aretaeus of Cappadocia and the first description of diabetes. Hormones. 2012;11(1):109-113. DOI: 10.1007/BF03401545
4. Davies MJ, Aroda VR, Collins BS, Gabbay RA, Green J, Maruthur NM, Rosas SE, Del Prato S, Mathieu C, Mingrone G, Rossing P, Tankova T, Tsapas A, Buse JB. Management of hyperglycaemia in type 2 diabetes, 2022. A consensus report by the American diabetes association (ADA) and the European association for the study of diabetes (EASD). Diabetol. 2022;45(11):1925-1966. DOI: 10.1007/s00125-022-05787-2
5. Haythorne E, Lloyd M, Walsby-Tickle J, Tarasov AI, Sandbrink J, Portillo I, Exposito RT, Sachse G, Cyranka M, Rohm M, Rorsman P, McCullagh J, Ashcroft FM. Altered glycolysis triggers impaired mitochondrial metabolism and mTORC1 activation in diabetic β-cells. Nat Commun. 2022;6754(2022). DOI: 10.1038/s41467-022-34095-x
6. Kahn CR, Weir GC, King GL, Moses AC, Smith RJ, Jacobson AM. Joslin's diabetes mellitus. 14th ed. Philadelphia: Lippincott Williams & Wilkins; 2004. 1224 p.
7. Edensor S, Jones O, Chakera AJ. Diagnosis and management of monogenic diabetes in pregnancy. Curr Diabetes Rev. 2023;19(2):28-42. DOI: 10.2174/1573399818666220514153021
8. O'Rahilly S, Farooqi IS. Obesity, Diabetes mellitus, and metabolic syndrome. In: Loscalzo J, editor. Harrison's principles of internal medicine. New York: McGraw-Hill Co. Inc.; 2022. 3080-3156 p.
9. Ali G, Subhan F, Abbas M, Zeb J, Shahid M, Sewell RD. A streptozotocin-induced diabetic neuropathic pain model for static or dynamic mechanical allodynia and vulvodynia: Validation using topical and systemic gabapentin. Naunyn-Schmiedeb Arch Pharmacol. 2015;388(11):1129-40. DOI: 10.1007/s00210-015-1145-y
10. Islam MS. Experimental rodent models of type 2 diabetes: A review. Methods Find Exp Clin Pharmacol. 2009;31(4):61-249. DOI: 10.1358/mf.2009.31.4.1362513
11. Federiuk IF, Casey HM, Quinn MJ, Wood MD, Ward WK. Induction of type-1 diabetes mellitus in laboratory rats by use of alloxan: Route of administration, pitfalls, and insulin treatment. Comp Med. 2004;54(3):252-7. [available at]
12. Kamli-Salino SJ, Brown PJ, Haschler TN, Liang L, Feliers D, Wilson HM, Delibegovic M. Induction of experimental diabetes and diabetic nephropathy using anomer-equilibrated streptozotocin in male C57Bl/6J mice. Biochem Biophys Res Commun. 2023;650:109-116. DOI: 10.1016/j.bbrc.2023.01.089
13. Carmona M, Paco-Meza LM, Ortega R, Cañadillas S, Caballero-Villarraso J, Blanco A, Herrera C. Hypoxia preconditioning increases the ability of healthy but not diabetic rat-derived adipose stromal/stem cells (ASC) to improve histological lesions of streptozotocin-induced diabetic nephropathy. Pathol Res Pract. 2022;230:1-5. DOI: 10.1016/j.prp.2021.153756
14. Ismail HK, Al-Sabawy RA, Jumaa HJ. Protective effect of placental mesenchymal stem cells on histological changes of pancreas experimentally induced by alloxan in mice. Iraqi J Vet Sci. 2020;34:1-8. DOI: 10.33899/ijvs.2020.163563
15. Sarhat ER, Wadi SA, Sedeeq BI, Sarhat TR, Jasim NA. Study of histopathological and biochemical effect of *Punica granatum L*. extract on streptozotocin-induced diabetes in rabbits. Iraqi J Vet Sci. 2019;33:189-194. DOI: 10.33899/ijvs.2019.125523.1045
16. Ismail HK. Histopathological alterations of male and female reproductive systems induced by alloxan in rats. Iraqi J Vet Sci. 2020;35:223-226. DOI: 10.33899/ijvs.2020.126626.1351
17. Institute of Laboratory Animal Resources (US). Committee on Care and Use of Laboratory Animals, 1986. Guide for the care and use of laboratory animals (No. 86). US Department of Health and Human Services, Public Health Service, National Institutes of Health. [available at]
18. Ighodaro OM, Adeosun AM, Akinloye OA. Alloxan-induced diabetes, a common model for evaluating the glycemic-control potential of therapeutic compounds and plants extracts in experimental studies.

Medicina (Kaunas). 2017;53(6):365-374. DOI: 10.1016/j.medici.2018.02.001
19. Furman BL. Streptozotocin-induced diabetic models in mice and rats. Curr Protoc. 2021;1(4):1-21. DOI: 10.1002/cpz1.78
20. Dupas J, Goanvec C, Feray A, Guernec A, Alain C, Guerrero F, Mansourati J. Progressive induction of type 2 diabetes: Effects of a reality-like fructose enriched diet in young Wistar rats. PLoS One. 2016;11(1):1-13. DOI: 10.1371/journal.pone.0146821
21. Luna LG. Manual of histologic staining methods of the armed forces institute of pathology. 3rd ed. New York: McGraw-Hill; 1968. 28-38 p.
22. Suvarna K, Layton CH, Bancroft J. Bancroft's theory and practice of histological techniques. 8th ed. New York: Elsevier Press; 2018. 1-30 p.
23. Snedecor GW, Cochran WG. Statistical Methods. 7th ed. USA: Iowa State University; 1980. 507 p.
24. Hodrea J, Saeed A, Molnar A, Fintha A, Barczi A, Wagner LJ, Szabo AJ, Fekete A, Balogh DB. SGLT2 inhibitor dapagliflozin prevents atherosclerotic and cardiac complications in experimental type 1 diabetes. PLoS One. 2022;17(2):1-17. DOI: 10.1371/journal.pone.0263285
25. Eprintsev AT, Fedorin DN, Bakarev MY. Molecular and biochemical studies of succinate dehydrogenase in rat liver under conditions of alloxan diabetes. Biomed Khim. 2022;68(4):272-278. DOI: 10.18097/PBMC20226804272
26. Lenzen S. The mechanisms of alloxan- and streptozotocin-induced diabetes. Diabetol. 2008;2:216-26. DOI: 10.1007/s00125-007-0886-7
27. Szkudelski T. The mechanism of alloxan and streptozotocin action in B cells of the rat pancreas. Physiol Res. 2001;50(6):537-46. [available at]
28. Aluwong T, Ayo JO, Kpukple A, Oladipo OO. Amelioration of hyperglycaemia, oxidative stress and dyslipidemia in alloxan-induced diabetic Wistar rats treated with probiotic and vitamin C. Nutrients. 2016;8(5):151. DOI: 10.3390/nu8050151
29. Wang YL, Lin SX, Wang Y, Liang T, Jiang T, Liu P, Li XY, Lang DQ, Liu Q, Shen CY. p-Synephrine ameliorates alloxan-induced diabetes mellitus through inhibiting oxidative stress and inflammation via suppressing the NF-kappa B and MAPK pathways. Food Funct. 2023;14(4):1971-1988. DOI: 10.1039/d2fo03003a
30. Damasceno DC, Netto AO, Iessi IL, Gallego FQ, Corvino SB, Dallaqua B, Sinzato YK, Bueno A, Calderon IM, Rudge MV. Streptozotocin-induced diabetes models: Pathophysiological mechanisms and fetal outcomes. BioMed Res Int. 2014;2014:1-11. DOI: 10.1155/2014/819065
31. Camargo AC, Dos Santos SA, Rinaldi JC, Constantino FB, Colombelli KT, Scarano WR, Felisbino SL, Justulin LA. Streptozotocin-Induced maternal hyperglycemia increases the expression of antioxidant enzymes and mast cell number in offspring rat ventral prostate. Anat Rec. 2017;300(2):291-299. DOI: 10.1002/ar.23510
32. He W, Liu H, Hu L, Wang Y, Huang L, Liang A, Wang X, Zhang Q, Chen Y, Cao Y, Li S, Wang J, Lei X. Icariin improves testicular dysfunction via enhancing proliferation and inhibiting mitochondria-dependent apoptosis pathway in high-fat diet and streptozotocin-induced diabetic rats. Reprod Biol Endocrinol. 2021;19(1):168. DOI: 10.1186/s12958-021-00851-9
33. Simonyan RM, Simonyan KV, Simonyan GM, Khachatryan HS, Babayan MA, Danielyan MH, Darbinyan LV, Simonyan MA. Superoxide-producing thermostable associate from the small intestines of control and alloxan-induced diabetic rats: Quantitative and qualitative changes. BMC Endocr Disord. 2022;22:250. DOI: 10.1186/s12902-022-01160-x
34. Bhor VM, Raghuram N, Sivakami S. Oxidative damage and altered antioxidant enzyme activities in the small intestine of streptozotocin-induced diabetic rats. Int J Biochem Cell Biol. 2004;36(1):89-97. DOI: 10.1016/s1357-2725(03)00142-0
35. Refat NA, Abou El-Fattouh MS, Metwally MM, Khamis T, Abdalla MA. Curative and protective potentials of *Moringa oleifera* leaf decoction on the streptozotocin-induced diabetes mellitus in albino rats. Iraqi J Vet Sc. 2023;37(1):73-82. DOI: 10.33899/ijvs.2022.133509.2242
36. Kume E, Ohmachi Y, Itagaki S, Tamura K, Doi K. Hepatic changes of mice in the subacute phase of streptozotocin (SZ)-induced diabetes. Exp Toxicol Pathol. 1994;46:368-374. DOI: 10.1016/S0940-2993(11)80119-3
37. Honjo K, Doi K, Doi C, Mitsuoka T. Histopathology of streptozotocin-induced diabetic DBA/2N and CD-1 mice. Lab Anim. 1986;20(4):298-303. DOI: 10.1258/002367786780808695
38. Goel KA. Submassive necrosis of liver of *Channa gachua*, a freshwater fish during experimental alloxan diabetes. Anat Anz. 1977;141(2):130-135. [available at]
39. Lucchesi AN, Cassettari LL, Spadella CT. Alloxan-induced diabetes causes morphological and ultrastructural changes in rat liver that resemble the natural history of chronic fatty liver disease in humans. J Diabetes Res. 2015; 2015:1-11. DOI: 10.1155/2015/494578
40. Mahmoud AB, Al-Salahy MB. Physiological and histological studies on the effect of lupine seeds on the fish, *Clarias lazera* treated with glucose and alloxan. Fish Physiol Biochem. 2004;30:213-229. DOI: 10.1007/s10695-005-8243-6

دراسة نسجية مرضية مقارنة للبنكرياس والامعاء والكبد للجرذان المصابة بداء السكري التجريبي

ميعاد احمد علي[1] و نشأت غالب مصطفى[2]

[1]مديرية زراعة نينوى، [2]فرع الفسلجة والكيمياء الحياتية والأدوية، كلية الطب البيطري، جامعة الموصل، الموصل، العراق

الخلاصة

لعدة عقود كان الاستحداث التجريبي لداء السكري يمثل الركيزة الأساسية في بحوث هذا المرض. وهناك طرق متنوعة لاستحداث داء السكري ومنها الاستحداث بالمواد الكيميائية مثل الالوكسان والستربتوزوتوسين (لاستحداث النوع الأول)، او الاستحداث الجراحي باستئصال البنكرياس، أو باستخدام غذاء عالي الكربوهيدرات (لاستحداث النوع الثاني)، أو باستخدام حيوانات مصابة وراثيا بداء السكري مثل فئران اوبي/اوبي. ولكن هناك عدد قليل من الدراسات التي أنجزت لتقييم التغييرات النسجية المرضية لطرق الاستحداث المختلفة. لذلك كان الهدف من الدراسة الحالية هو استخدام الطرق الشائعة لاستحداث داء السكري من خلال حقن الالوكسان، الستربتوزوتوسين، وغذاء عالي الكاربوهيدرات في ذكور الجرذان البالغة. تركيز كلوكوز مصل الدم أثبت حدوث داء السكري، وأظهرت الدراسة النسجية المرضية مدى واسع من الآفات المرضية في البنكرياس (انخفاض معنوي) في عدد وأقطار جزر لانكرهانز) وفي الكبد (انتفاخ الخلايا الحاد، التنخر، وجود بقايا الخلايا، تحلل النواة، والتنكس الفجوي) وفي الأمعاء (انخفاض معنوي) في طول وعرض زغابات الأمعاء، وانخفاض في عدد الخلايا الكأسية). نستنتج من هذه الدراسة أن طرق استحداث داء السكري في الجرذان لها مدى واسع من الآفات النسجية المرضية.